An interpretation and modification of the SWT function

Daniel Kujawski[1]
Mechanical and Aerospace Engineering
Western Michigan University, 1903 W. Michigan Ave.
Kalamazoo, MI 49008-4353, USA

ABSTRACT

In this paper a new interpretation and modification of the SWT function in terms of the total damaging energy density is proposed and discussed. The total damaging energy density is the sum of the damaging part of the strain energy density and complementary energy density corresponding to the first quadrant in damaging σ_D-ε_D axes. For cyclic loading with positive mean stress ($\sigma_m \geq 0$) the proposed function reduces to the original SWT formulation. For cyclic loading with negative mean stress ($\sigma_m < 0$) the maximum stress is augmented by 1/3 of absolute value of the mean stress. The proposed approach shows a consistent correlation of the mean stress effects for both positive and negative mean stresses.

Key words: Modified SWT function, total energy density, fatigue life, R-ratio effects

1.0 INTRODUCTION

It is well known that uniaxial fatigue loading is highly affected by a normal mean stress $\sigma_m = (\sigma_{min} + \sigma_{max})/2$ or a stress ratio $R = \sigma_{min}/\sigma_{max}$ where: σ_{min} and σ_{max} are the minimum and the maximum stresses, respectively. The same stress amplitude, σ_a together with a positive mean stress, $\sigma_m > 0$, will result in a shorter fatigue life in comparison if a mean stress is negative, $\sigma_m < 0$. In general, $\sigma_m > 0$ is detrimental whereas $\sigma_m < 0$ is beneficial [1-2]. The most widely used methods for accounting of mean stress effects are Morrow [3] and SWT [4] approaches.

In a stress-based formulation they are represented as:

- Morrow $$\sigma_{ar} = \frac{\sigma_a}{1 - \sigma_m/\sigma'_f} \quad (1)$$

- SWT $$\sigma_{ar} = \sqrt{\sigma_{max}\sigma_a} \quad (2)$$

where σ_{ar} is an equivalent fully-reversed stress amplitude and σ'_f is a fatigue strength coefficient.

[1]Corresponding author. Email address: daniel.kujawski@wmich.edu

Figures 1 and 2 illustrates how the above Eqs. (1) and (2) correlate R-ratio effect for ductile iron [5] and 7075-T651 Al alloy [6], respectively. For both materials, Eq. (1) results in a nonconservative life estimation for R > -1 and too conservative estimation for R < -1 in comparison to a fully reversed loading with R = -1. On the other hand, Eq. (2) provides a fairly good estimation for loadings at R > -1 associated with $\sigma_m > 0$ and a nonconservative estimation for R < -1.5 corresponding to $\sigma_m < 0$ when compared to R = -1. Comprehensive data for 7075-T651 Al alloy [6] are ranging from 8 to $2x10^6$ reversals $2N_f$ to failure and clearly indicate two distinct slopes: a lower slope for $2N_f < 2{,}000$ and another higher one for $2N_f > 2{,}000$ reversals, as it is seen in Fig. 2. It is interesting to note, that data for $2N_f < 2{,}000$ exhibit very narrow scatter in terms of the equivalent σ_{ar} calculated using both approaches.

Customarily, Morrow relation is more widely known as a strain-based approach [3] and is represented by Eq. (3), whereas the SWT approach as a stress-strain function in the form of Eq. (4) as it was originally proposed in Ref. [4].

- Morrow $$\varepsilon_a = \frac{\sigma'_{f-\sigma_m}}{E}\left(2N_f\right)^b + \varepsilon'_f\left(2N_f\right)^c \quad (3)$$

- SWT $$\sigma_{max}\varepsilon_a = \frac{\sigma'^2_f}{E}\left(2N_f\right)^{2b} + \sigma'_f\varepsilon'_f\left(2N_f\right)^{b+c} \quad (4)$$

where: E is the elastic modulus, ε'_f is a fatigue ductility coefficient, *b* and *c* are fatigue strength and fatigue ductility exponents, respectively.

Figures 3a and 3b illustrate how the above relations (3) and (4) correlate R-ratio effect for ductile iron and 7075-T651 Al alloy, respectively. For both materials, Eq. (3) results in a nonconservative life estimation for R > -1 and a relatively good estimation for R < -1. On the other hand, Eq. (4) provides a good estimation for R > -1 (associated with $\sigma_m > 0$) and a nonconservative estimation for R < -1.5 (corresponding to $\sigma_m < 0$). Such inconsistent

(conservative and nonconservative) correlations with respect to R-ratios for Morrow and the SWT approaches have been often reported in the literature [1-2, 5-11]. In the past, a several attempts have been made to modified Morrow and SWT approaches [e.g. 12-16].

By comparing Morrow and the SWT correlations depicted in Figs. 1, 2, 3 and 4 it can be concluded that except data for R < -1 (or $\sigma_m < 0$), the SWT function provides more consistent correlation than Morrow in both the stress or the strain and stress-strain based formulations.

The aim of this paper is to propose a new interpretation and modification of the SWT function in terms of the total damaging energy density. This modified SWT function provides a sound physical interpretation and eliminates its nonconservative correlation related to R<-1. Also, the better understanding of its intrinsic virtues would shade the light how the modified SWT function can be extended to multiaxial loading situations.

2.0 BAGRAUND

2.1 Strain energy density and complementary energy density in monotonic loading

Let consider a material with a non-linear stress-strain behavior given by Eq. (5)

$$\sigma = H\,\varepsilon^{n} \tag{5}$$

where H is a strength coefficient and n is a strain hardening exponent.

For the material given by Eq. (5) the strain energy density W_S and the complementary energy density W_C can be computed as:

$$W_S = \int_0^{\varepsilon} \sigma\, d\varepsilon = \int_0^{\varepsilon} H\,\varepsilon^{n}\, d\varepsilon = \frac{H}{1+n}\left(\varepsilon^{n}\right)^{1+n} = \frac{\sigma^{1}\varepsilon^{1}}{1+n} \tag{6}$$

and

$$W_C = \int_0^{\sigma * ¿ \left(\frac{\sigma}{H}\right)^{1/n} d\sigma = \frac{1}{H^{1/n}} \frac{(\sigma^2)^{1+1/n}}{1+1/n} = \frac{n}{1+n} \sigma^{¿} \varepsilon^{¿}} ¿ ¿ ¿ ¿ \quad (7)$$

It is seen from Eqs. (6) and (7) that for a linear material $n=1$ and $W_S = W_C$.

Figure 4 illustrate both energies W_S and W_C under monotonic loading for a hypothetical material with a non-linear stress-strain behavior. The sum of W_S and W_C is the total energy density W given by Eq. (8).

$$W = W_S + W_C = \sigma^{¿} \varepsilon^{¿} \quad (8)$$

2.1 Strain energy density and complementary energy density in cyclic loading and their relation to the SWT function

Figure 5 depicts a fully reversed stabilized elastic-plastic hysteresis loops. It can be noted that the total energy density, W, given by Eq. (8) can be calculated only in the first or third quadrants. From fatigue damage viewpoint, only the total energy density at the first quadrant can contribute to energy release associated with new crack surface formation. The total energy density from the third quadrant may contribute to fatigue damage but cannot contribute to energy realize rate since crack flanks are held in contact under compressive stress. For fully reversed loading, cyclic strains and stresses are going back and forth symmetrically with respect to the σ and ε axes having their origin at zero. Therefore, for fully reversed loading the σ and ε axes are overlap with damaging axes σ_D and ε_D as it is shown in Fig. 5. Hence, it is postulated that:

"*only the total energy density associated with the first quadrant in the* σ_D-ε_D *axes contribute to fatigue damage* W_D*"*.

$$W_D = W_S + W_C \; when \; both \; \sigma_D \geq 0 \wedge \varepsilon_D \geq 0 \quad (9)$$

The fatigue damage parameter W_D given by Eq. (9) can be calculated using a cyclic stress-strain curve shown in Fig.5. Figure 6a shows a stabilized hysteresis loop for $\sigma_m>0$, $\varepsilon_m>0$ and Fig. 6b depicts the case when $\sigma_m<0$and $\varepsilon_m<0$. For stabilized hysteresis loops dislocations move back and forth around $\pm\varepsilon_m$. Therefore, damaging $\sigma_D$axis would pass through ε_m whereas the ε_D and ε axes overlap (Fig. 6a). The total damaging energy density corresponding to $\sigma_D>0$ and $\varepsilon_D>0$ is given by Eq. (10).

$$W_D=W_S+W_C=\sigma_{max}\varepsilon_a \tag{10}$$

By comparing the LHS of Eq. (4) with the RHS of Eq. (10) it is seen that

$$SWT=W_D=\sigma_{max}\varepsilon_a \; valid \; for \; \sigma_m\geq 0 \tag{11a}$$

As it was mentioned earlier, the SWT function given by Eqs. (4) or (11a) correlates well a mean stress effects only when $\sigma_m\geq 0$ or $R\geq -1$. For cyclic loading with $\sigma_m<0$ or $R\leftarrow 1$ Eq. (11a) need to be modified. Experimental results for $\sigma_m<0$ or $R_\varepsilon\leftarrow 1$ (where strain ratio R_ε = minimum strain/ maximum strain) indicate that during an initial transient behavior hysteresis loops exhibit relaxation of the negative mean stresses as it is shown in Fig. 7 [17]. Typical stabilized hysteresis loops for tests at strain ratio R_ε =-2 result in a stabilized mean stress equal 1/3 of the initial value of σ_m. Therefore, to account for such effects associated with $\sigma_m<0$ the maximum stress is augmented by a stabilized part of the mean stress $|\sigma_m|/3$ and the SWT function given by Eq. (11a) will be modify to Eq. (11b), called mSWT .

$$mSWT=W_D=(\sigma_{max}+|\sigma_m|/3)\varepsilon_a \; valid \; for \; \sigma_m<0 \tag{11b}$$

Figure 6b illustrates how Eq. (11b) is calculated with respect to σ_D and ε_D axes shown by dashed lines. It can be noted that Eq. (11a) for $\sigma_m\geq 0$ (or $R\geq -1$¿ coincide with the original formulation of the SWT function [4], whereas Eq. (11b) for $\sigma_m<0$ (or $R\leftarrow 1$¿ represents the modified SWT function called mSWT.

In terms of the equivalent fully reversed stress amplitude σ_{ar}, Eq. (2) would take the following forms:

$$\sigma_{ar} = \sqrt{\sigma_{max}\sigma_a} \qquad valid\ for\ \sigma_m \geq 0 \tag{12a}$$

and

$$\sigma_{ar} = \sqrt{(\sigma_{max} + |\sigma_m|/3)\sigma_a} \qquad valid\ for\ \sigma_m < 0 \tag{12b}$$

where Eq. (12b) is called the stress-based mSWT function.

3.0 COMPARISON WITH EXPERIMENTAL DATA

Figure 8 shows how the mSWT function given by Eq. (11) correlates R-ratio effect for 7075-T651 Al alloy [6]. Data for R > -1 and R < -1 coalesce within the narrow scatter band corresponding to fully reversed loading data at R = -1. The mSWT function successfully corrects R < -1 data and eliminates the nonconservative correlation stipulated by the original SWT function (Fig.4). Similarly, Figs. 9a and 9b show how mSWT function given by Eq. (12) correlates R-ratio effect for ductile iron [5] and 7075-T651 Al alloy [6], respectively. For both materials, data for R > -1 and R < -1 consolidate to a narrow band together with the fully reversed loading data at R = -1. Zhao and Jiang [6] reported also, for dogbone samples, a fracture angle with respect to specimen's axis. For $2N_f$ < 2,000 fracture surface angles were ranging from 35° to 45° (close to shear fracture), whereas for $2N_f$ > 2,000 the fracture surfaces were almost normal to the sample axis with an average angle between 0° to 5°. Therefore, it can be stated that a double slope in Fig. 9b is associated with different failure modes observed experimentally [6].

4.0 DISCUSSION

Comprehensive experimental data for 7075-T651 Al alloy [6] include also a two-step test results where the first step was conducted under fully compression-compression loading (σ_{max} < 0 with a number of cycles ranging from 4x10^5 to 10^6) and then switched to zero-to-tensile loading (R = 0) with σ_a = 100 MPa cycled till failure. By applying the second step alone, it would result in a fatigue life longer than 10^7 cycles. The number of cycles to failure in the second steps were affected by a fatigue damage cumulated in the first step and were ranging from 52 to 49,000 cycles. The second step with a small maximum positive stress σ_{max} = 200 MPa was necessary to fracture the specimens previously cycled in the first step with σ_{max} < 0. These two-step test results were correlated using Eqs. (11b) and (12b) as it is depicted in Fig. 10 together with data for R = -1. In Fig. 9 the number of reversals to failure $2N_f$ was calculated as the sum of the reversals in the first and second steps. It is seen from Fig. 9 that the proposed mSWT function given by Eq. (11b) and (12b) is capable to quantify fatigue damage induced by compression-compression loading with σ_{max} < 0.

Recently, Oh and Akiniwa [18] successfully correlated positive mean stress effect on fatigue life of a pre-strain stainless-steel corner sheet using an apparent fully reversed stress amplitude σ'_{ar} calculated by the following SWT function

$$\sigma'_{ar} = \sqrt{E\varepsilon_a \sigma_{max}} \quad \text{for } \sigma_m \geq 0 \tag{13a}$$

To corelate the effect of negative mean stresses the above relation need to be modified to

$$\sigma'_{ar} = \sqrt{E\varepsilon_a \left(\sigma_{max} + \frac{|\sigma_m|}{3}\right)} \quad \text{for } \sigma_m < 0 \tag{13b}$$

Figure 11 shows the correlation of R-ratio effect on fatigue behavior of 7075-T651 Al alloy [6] using an apparent σ'_{ar} calculated by modified SWT function, Eq. (13). All data points are collapsed into a narrow scatter band with a single slope. Hence, Eq. (13) and the corresponding Fig. 10 provide a useful correlation but do not distinguish different failure modes as it is reflected by a double slope in Figs. 9b and 10b.

It can be interestingly pointed out that the total damaging energy density W_D and its relation to SWT function bares similarity to Neuber's rule [19], which relates nominal and actual total energy densities for notches as follows

$$\left(\frac{\sigma_{nom}^2}{E}\right) k_t^2 = \sigma\varepsilon \qquad (14)$$

where $\left(\frac{\sigma_{nom}^2}{E}\right)$ is the nominal elastic total energy density, k_t is a theoretical stress concentration factor, and $\sigma\varepsilon$ is the actual elastic-plastic total energy density at the notch root.

5.0 CONCLUSIONS

Based on the presented analyses the following conclusions can be drawn:

- Modified Smith-Watson-Topper function, mSWT, represents the total damaging energy density in the first quadrant of the damaging axes σ_D and ε_D.
- For cyclic loading with $\sigma_m \geq 0$ the proposed interpretation coincides with the original SWT parameter.
- For loading with $\sigma_m < 0$, the applied σ_{max} is augmented by $|\sigma_m|/3$.

Funding
The author received no financial support for the research, authorship, and/or publication of this article.

Declaration of Competing Interest

The author declare that he has no competing financial interest that could influence the work reported in this paper.

References

1. Stephens RI, Fatemi A, Stephens AA, Fuchs HO. Metal fatigue in engineering. John Wiley, 2001.
2. Dowling NE, Kampe SL, Kral MV. Mechanical Behavior of Material, Engineering Methods for Deformation, Fracture, and Fatigue, 5th edition, Pearson, 2019.
3. Morrow J. Fatigue properties of metals, section 3.2. In: Fatigue Design handbook, Pub. No. AE-4. Soc. of Automotive Engineers, Warrendale, PA, 1968. Section 3.2 is a summary

of a paper presented at division 4 of the SAE Iron and Steel Technical Committee, Nov. 4, 1964.

4. Smith KN, Watson P, and Topper TH. A stress-strain function for the fatigue of metals, Journal of Materials, ASTM, 1970, vol.5, no. 4, pp.767-778.
5. Meyer NM. Effects of mean stress and stress concentration on fatigue behavior of ductile iron. MSc Thesis in Mechanical Engineering, The University of Toledo, 2014.
6. Zhao T, Jiang Y. Fatigue of 7075–T651 aluminum alloy. International Journal of Fatigue, 2008, vol. 30, pp. 834-849.
7. Dowling NE. Mean stress effects in stress-life and strain-life fatigue. In: 2nd SAE Brazil International Conference on Fatigue, São Paulo, Brazil, SAE Paper No.2004–01-2227, SAE, 2004.
8. Dowling NE. Mean stress effects in strain-life fatigue, Fatigue and Fracture of Engineering Materials and Structures, 2009, vol. 32(12), pp. 1004–1019.
9. Fatemi A, Stephens RI. Tensile mean stress effects on uniaxial fatigue behaviour of 1045HR steel. Proc Int Conf on Fatigue and Fatigue Thresholds. Charlottesville, VA, EMAS, Warley, UK, 1987, pp. 537–46, 1987.
10. Wehner T, Fatemi A. Effects of mean stress fatigue behavior of a hardened carbon steel, International Journal of Fatigue, 1991, vol. 13(3), pp. 241–248.
11. Fang D, Berkovits A. Mean stress models for low cycle fatigue of a nickel-based superalloy. International Journal of Fatigue, 1994, vol. 16, pp.429–437.
12. Kujawski D and Ellyin F. A Unified approach to mean stress effect on fatigue threshold conditions, International Journal of Fatigue, 1995, vol.17(2), pp. 101-106.
13. Ince A., Glinka G., A modification of Morrow and Smith-Watson-Topper mean stress correction models. Fatigue and Fracture of Engineering Materials and Structures, 2011, vol. 34, pp. 854–67.
14. Kujawski D. A deviatoric version of the SWT parameter. International Journal of Fatigue, 2014, vol. 67, pp. 95–102.
15. Ince A. A mean stress correction model for tensile and compressive mean stress fatigue loadings. Fatigue and Fracture of Engineering Materials and Structures, 2017, vol. 40(6), pp. 939–48.

16. Ince A. A generalized mean stress correction model based on distortional strain energy, International Journal of Fatigue, 2017, vol. 104, pp. 273–282.
17. Koh SK, Stephens RI. Mean stress effects on low cycle fatigue for a high strength steel, Fatigue and Fracture of Engineering Materials and Structures, 1991, vol. 14, pp. 413–28.
18. Oh G, Akiniwa Y. Mean and residual stress effects on fatigue behavior in a pre-strained corner of stainless steel sheet, International Journal of Fatigue, 2021, vol. 145, 106125.
19. Neuber H. Theory of stress concentration for shear strained prismatic bodies with arbitrary non linear stress strain law, Trans. ASME, Journal of Applied Mechanics. 1961, pp. 544–555.

Figures

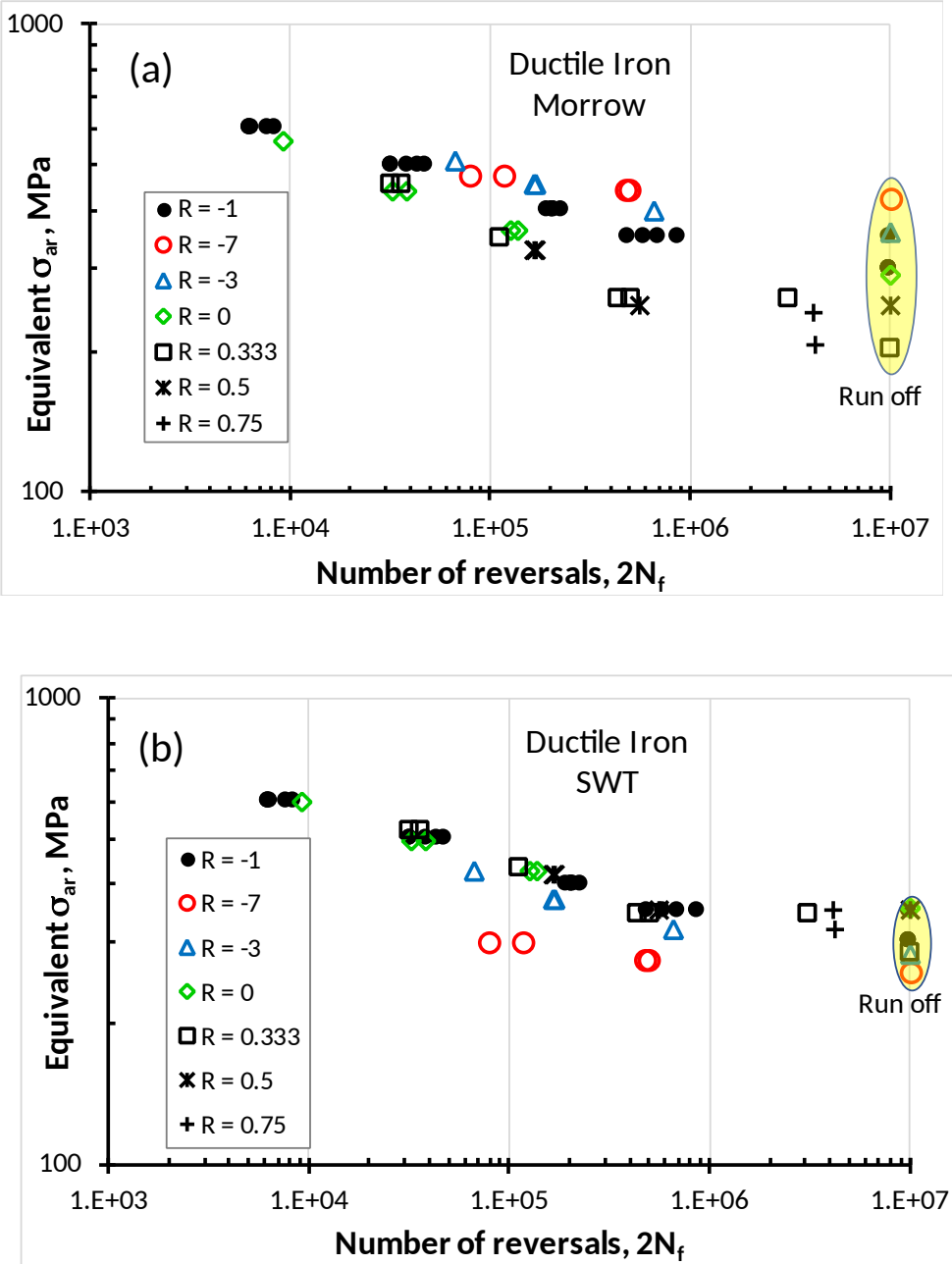

Figure 1 Stress-based correlation of R-ratio effect on fatigue behavior of ductile iron [5] using (a) Morrow approach, Eq. (1) and SWT function, Eq. (2).

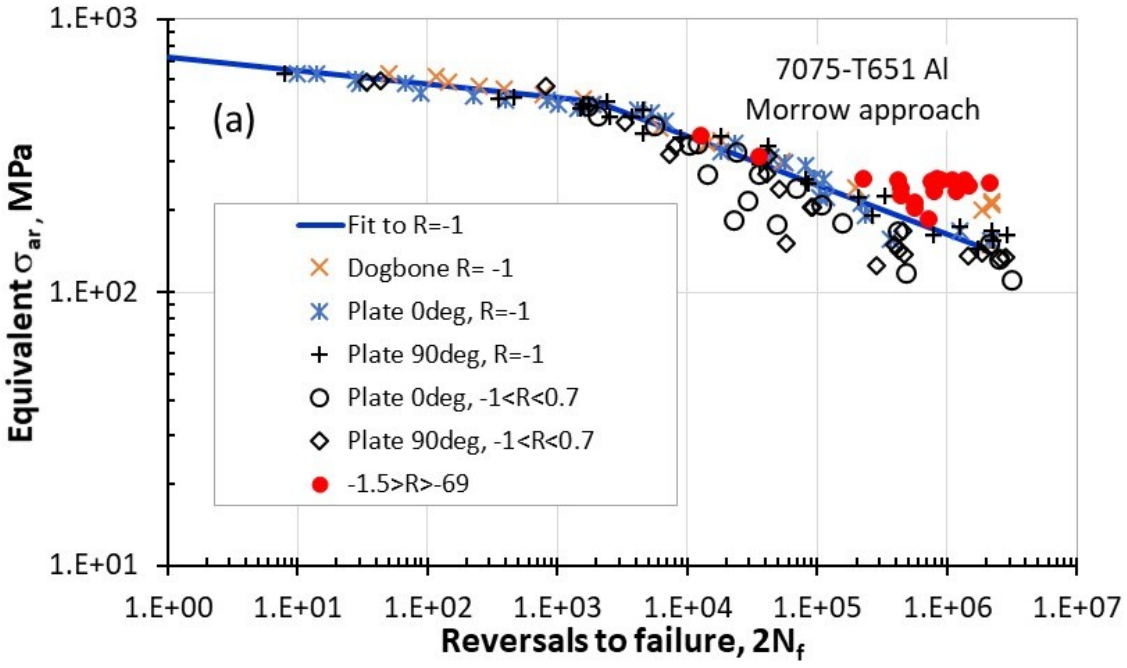
1.E+03
1.E+02
1.E+01
Equivalent σ_{ar}, MPa
(a)
7075-T651 Al
Morrow approach
Fit to R=-1
Dogbone R= -1
Plate 0deg, R=-1
Plate 90deg, R=-1
Plate 0deg, -1<R<0.7
Plate 90deg, -1<R<0.7
-1.5>R>-69
1.E+00
1.E+01
1.E+02
1.E+03
1.E+04
1.E+05
1.E+06
1.E+07
Reversals to failure, $2N_f$

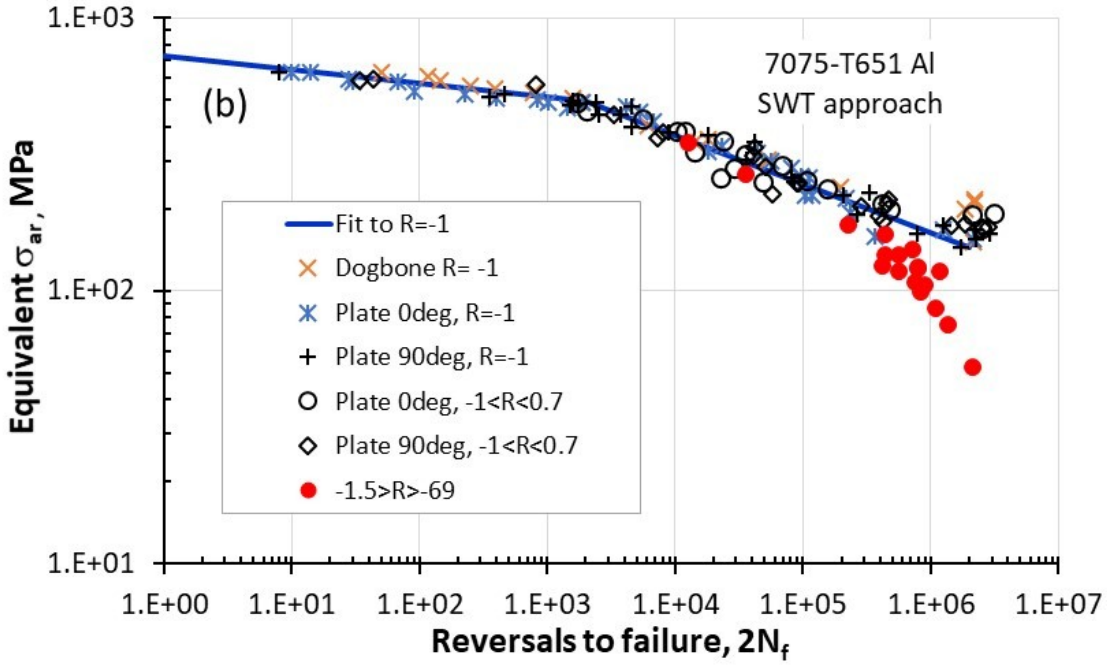

Figure 2 Stress-based correlation of R-ratio effect on fatigue behavior of 7075-T651 Al alloy [6] using (a) Morrow approach, Eq. (1) and SWT function, Eq. (2).

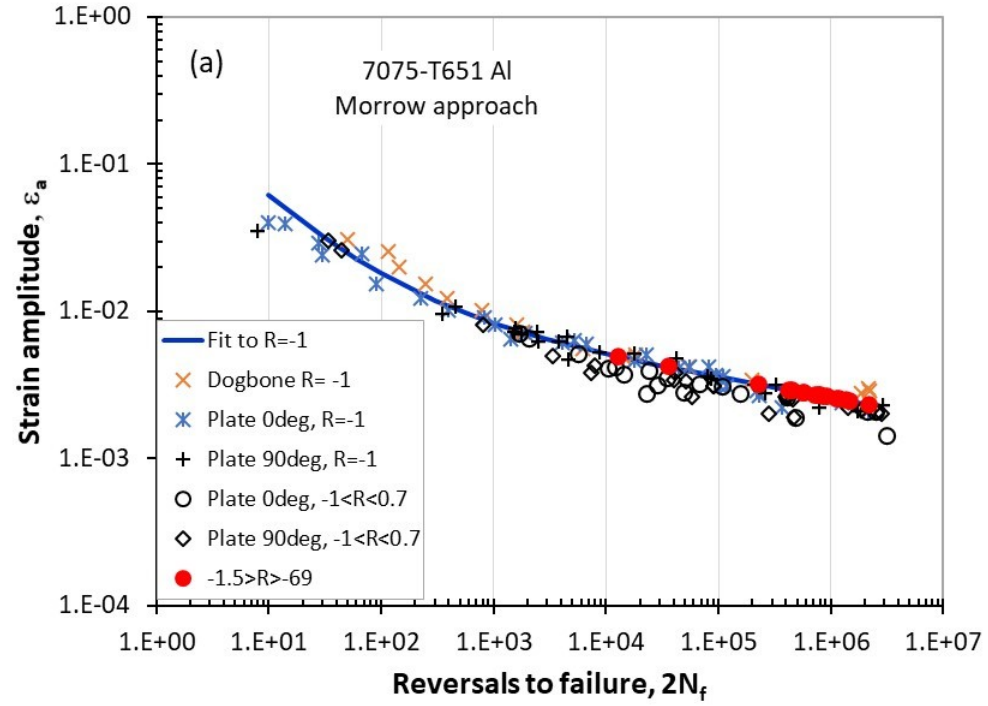

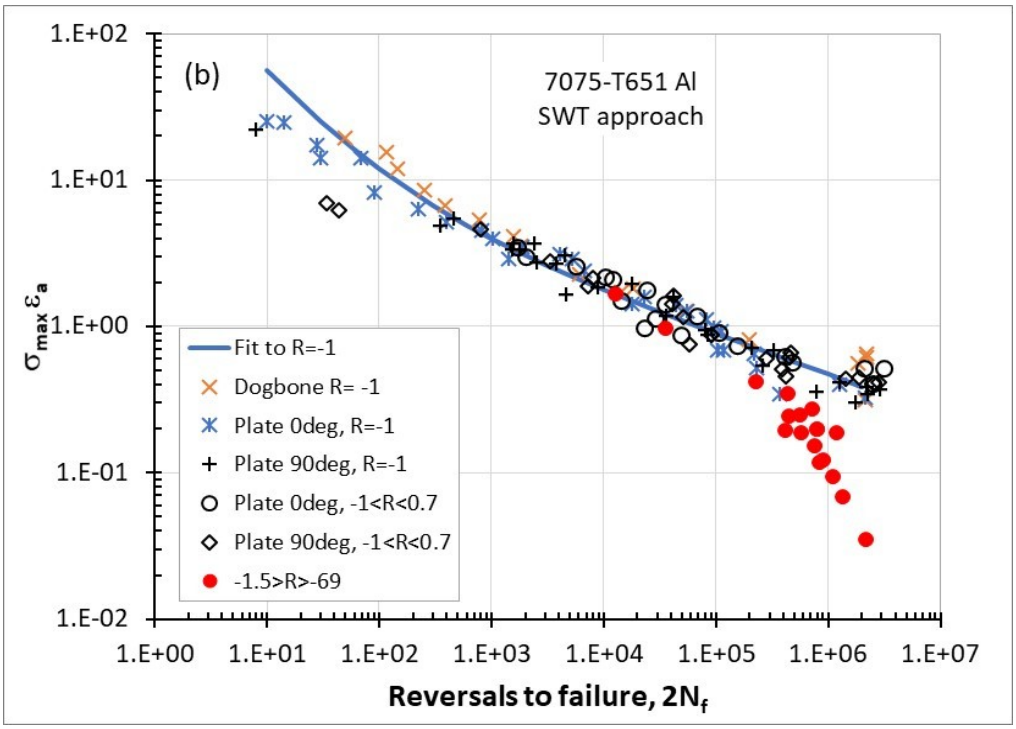

Figure 3 Correlation of R-ratio effect on fatigue behavior of 7075-T651 Al alloy [6] using (a) Morrow approach, Eq. (3) and SWT function, Eq. (4).

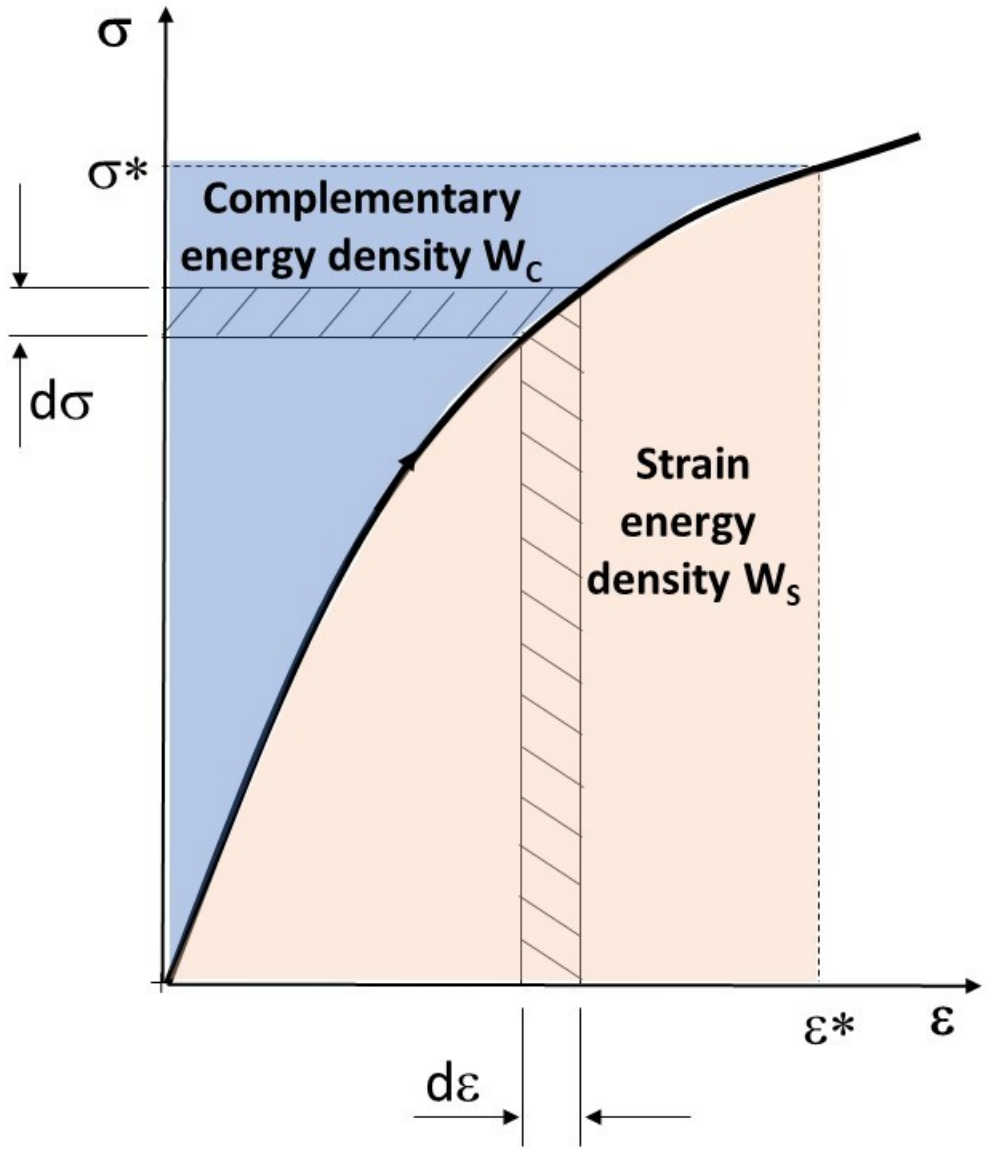

Figure 4 An illustration of a strain energy density W_S and a complementary energy density W_C for non-linear material.

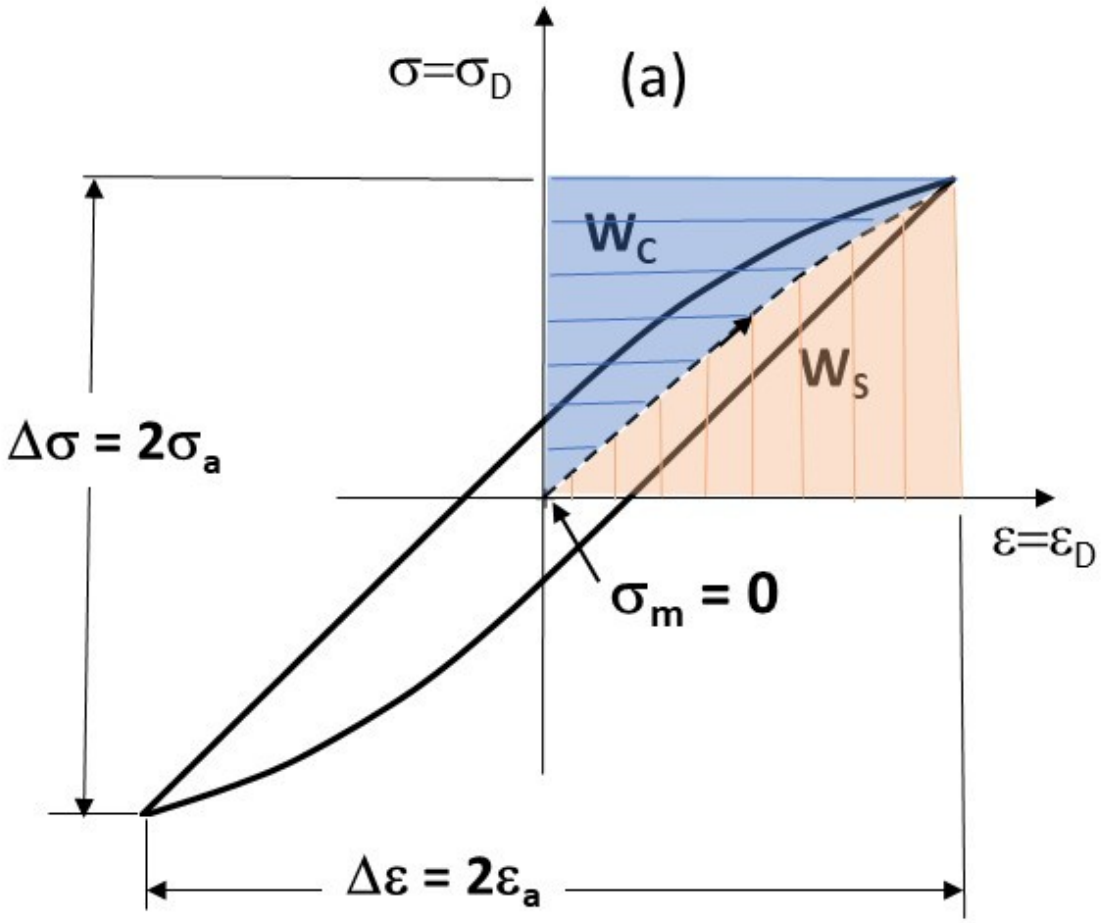

Figure 5 Illustration of the damaging energy density, $W_D = W_S + W_C = \sigma_a \varepsilon_a$ using cyclic stress-strain curve.

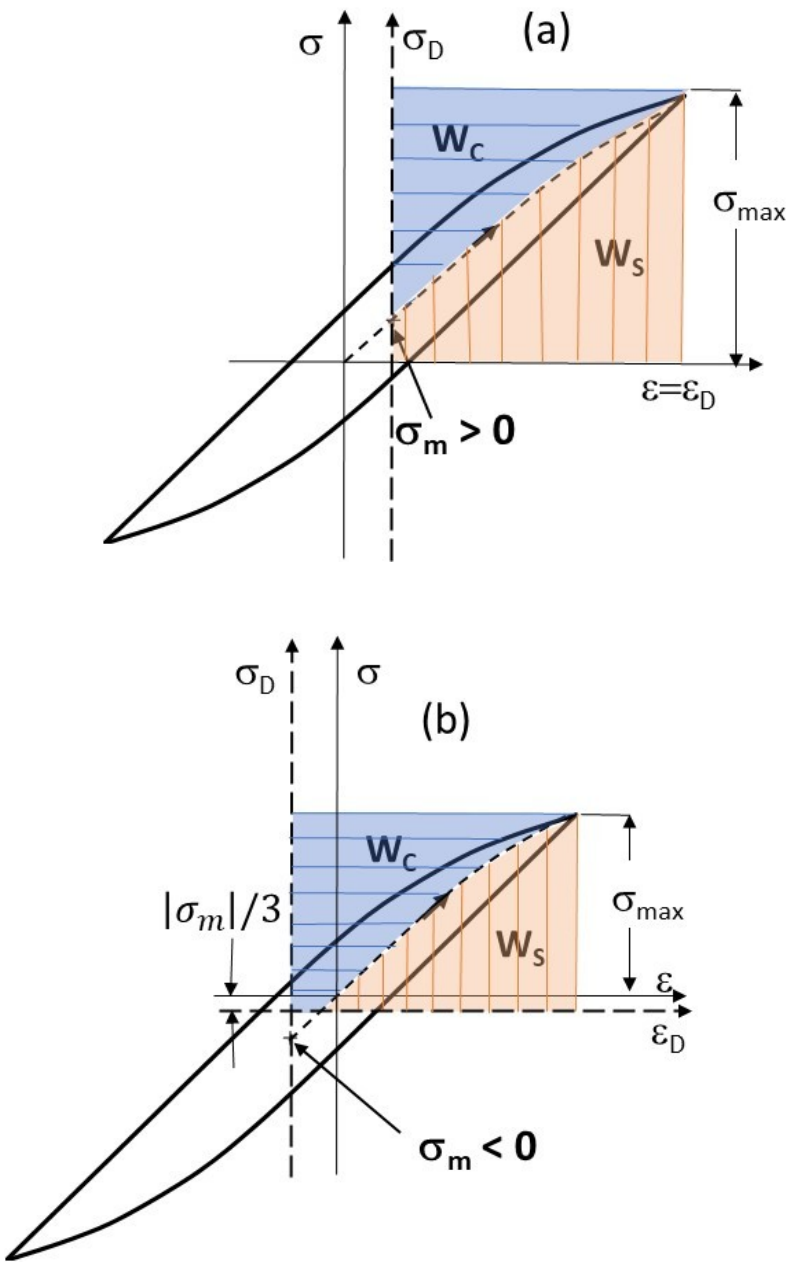

Figure 6 An illustration how the damaging energy density $W_D = W_S + W_C$ is determined for (a) cyclic loading with $\sigma_m > 0$ and (b) cyclic loading with $\sigma_m < 0$.

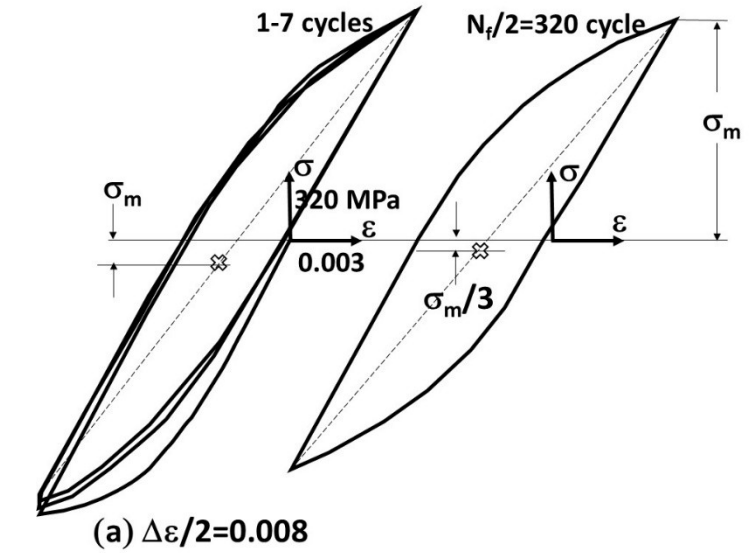

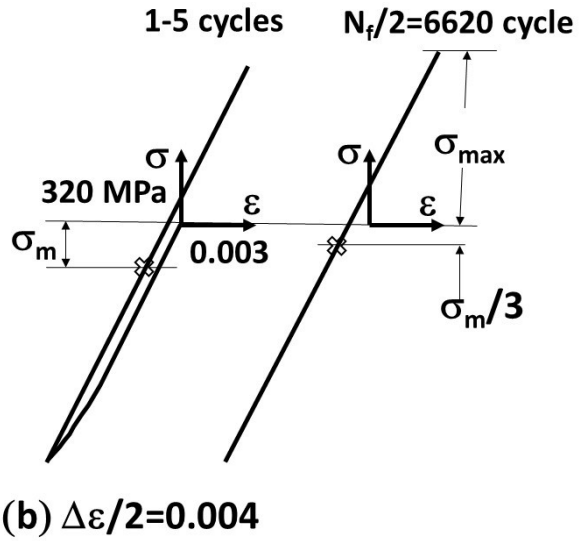

Figure 7 Typical hysteresis loops for R_ε = -2 [17] (⊠ is the center of the hysteresis loop).

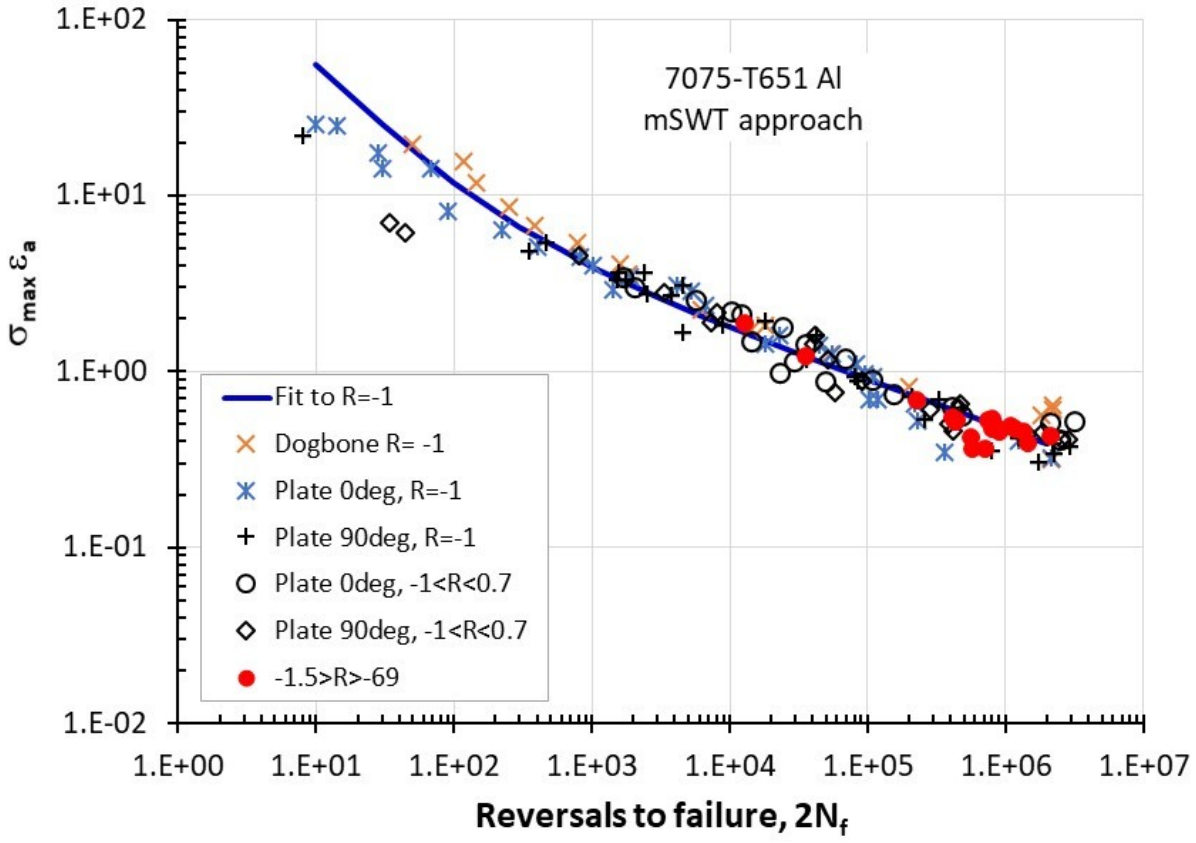

Figure 8 Correlation of R-ratio effect on fatigue behavior of 7075-T651 Al alloy [6] using mSWT function, Eqs. (11a) and (11b).

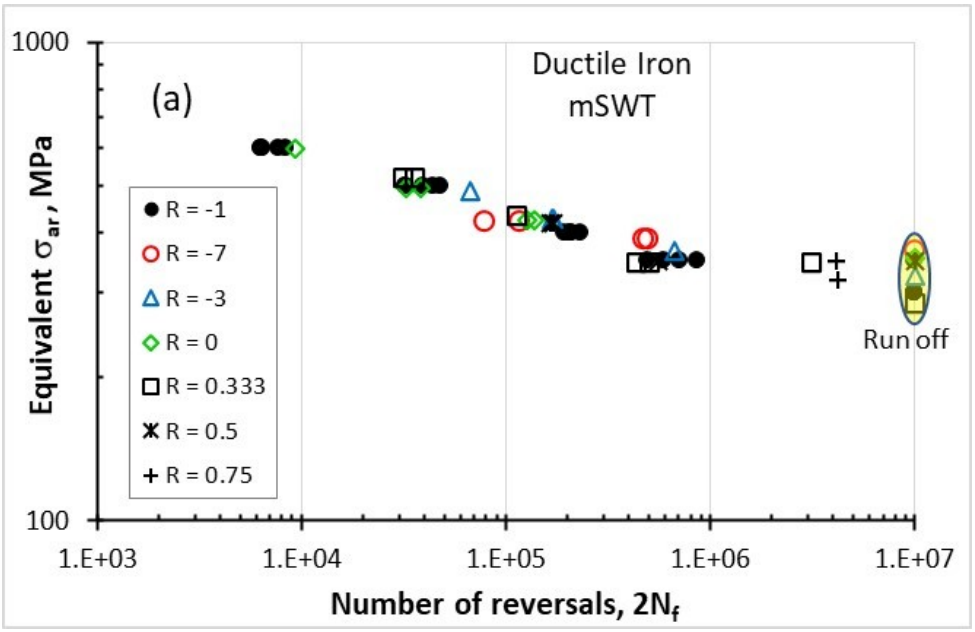

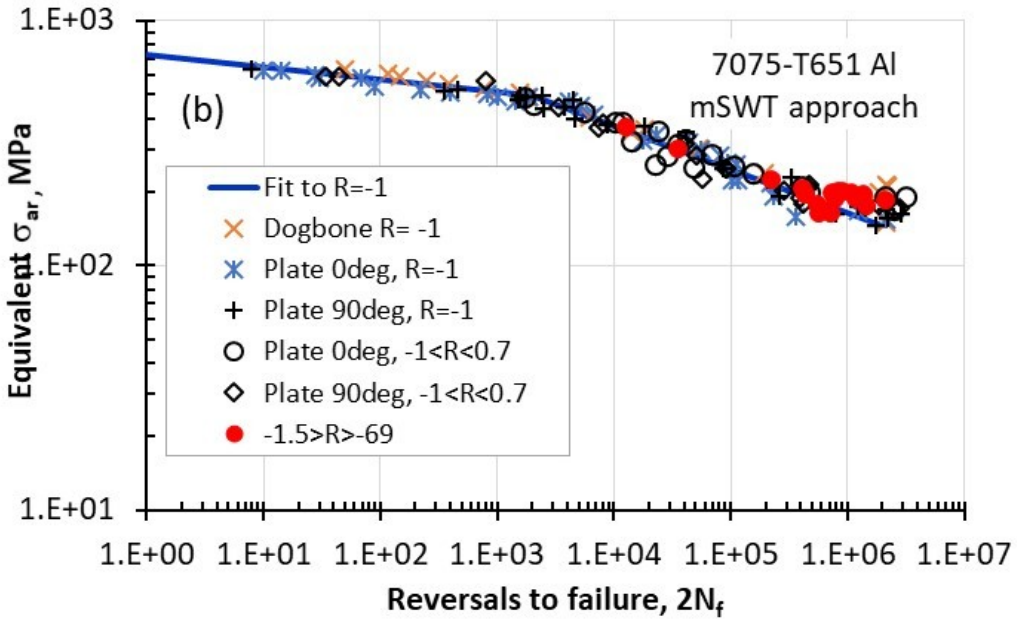

Figure 9 Stress-based correlation of R-ratio effect on fatigue behavior of (a) ductile iron [5] and (b) 7075-T651 Al alloy [6] using mSWT function, Eqs. (12a) and (12b).

(a)

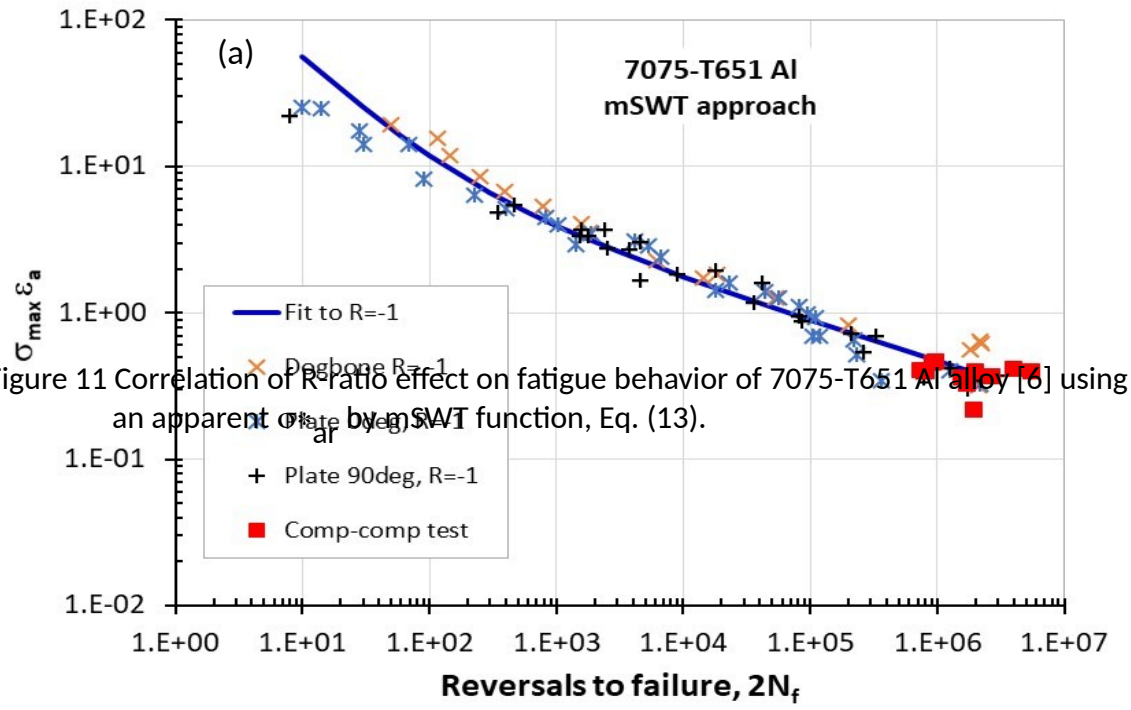

Figure 11 Correlation of R-ratio effect on fatigue behavior of 7075-T651 Al alloy [6] using an apparent σ_{ar} by mSWT function, Eq. (13).

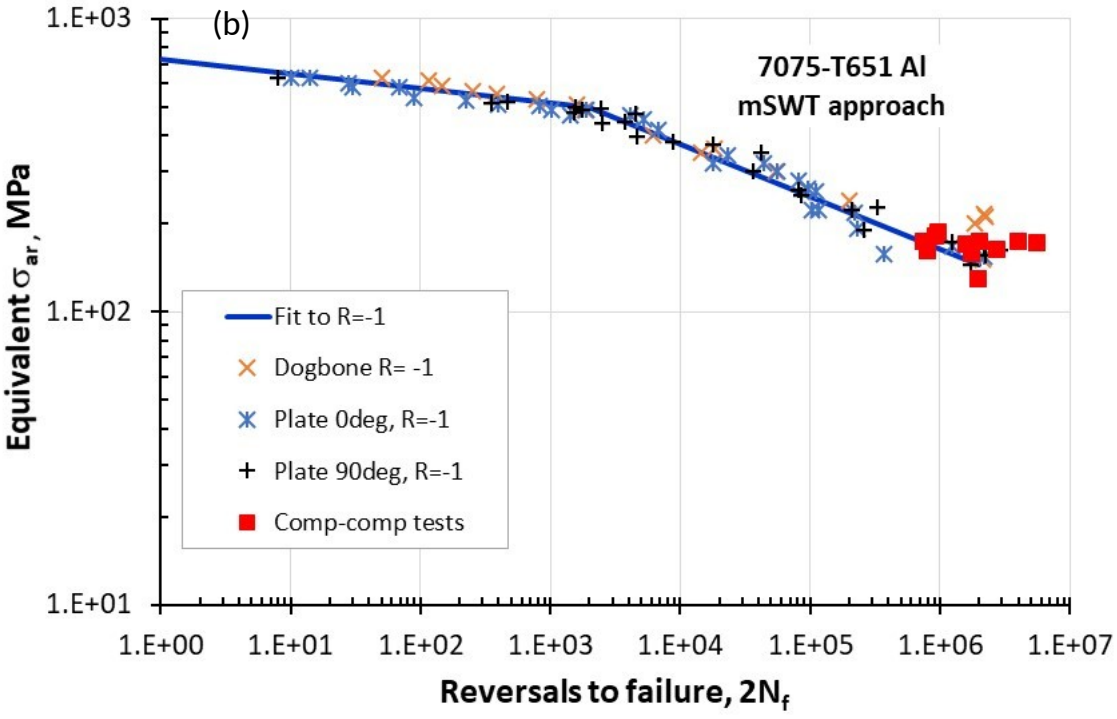

Figure 10 Correlation of two-step compression-compression test of 7075-T651 Al alloy [6] using mSWT function (a) Eq. (11b) and (b) Eq. (12b).